Available online at www.sciencedirect.com
SCIENCE DIRECT®
Pergamon
Cement and Concrete Research 34 (2004) 2209–2214
CEMENT AND CONCRETE RESEARCH

Alkali reactivity of mortars containing chert and incorporating moderate-calcium fly ash

F. Bektas[a], L. Turanli[a,*], T. Topal[b], M.C. Goncuoglu[b]

[a]Department of Civil Engineering, Middle East Technical University, 06531 Ankara, Turkey
[b]Department of Geological Engineering, Middle East Technical University, 06531 Ankara, Turkey

Received 12 December 2002; accepted 10 February 2004

Abstract

This paper reports the results of an experimental program, which aimed to investigate the alkali reactivity of chert and the effect of a moderate-calcium fly ash on the alkali–silica reaction. To determine the expansions, mortar bars were cast and tested in accordance with ASTM C1260. Mortar aggregate was replaced by chert, in controlled amounts, to find out the pessimum limit, if any. To evaluate the degree of cracking, sonic pulse velocity measurements and petrographic analysis were carried out on the cracked bars and on the thin sections taken from these bars, respectively. In the next series of tests, limestone and chert were blended together as mortar aggregate and cement was replaced by different dosages of fly ash to examine the changes in the mortar bar expansion as well as in the chemistry of reaction products. Microstructural observations were done on polished sections using a scanning electron microscope, equipped with energy dispersive X-ray analysis. The results showed that the chert used in this investigation had a pessimum proportion in the range of 5–15%. Sufficient fly-ash additions suppressed the expansion caused by chert. The study also revealed out that as the CaO/Na_2O_{eq} of alkali–silica gel increased, the expansivity of the gel decreased.

Keywords: Alkali–silica reaction; Chert; Pessimum proportion; Fly ash

1. Introduction

It is well known that chert can be an alkali-reactive constituent in concrete aggregate. In the published literature, numerous cases of alkali–silica reaction involving chert have been reported from countries around the world, such as Japan, United Kingdom, and North America [1].

The mineralogical composition of cherts varies from very fine-grained opaline silica to cryptocrystalline silica and from chalcedony to microcrystalline quartz [2]. These poorly crystallized forms of silica are all prone to hydroxyl ion attack, thus causing the dissolution of the aggregate. This triggers the formation and expansion of the alkali–silica gel and results in the cracking of the concrete. The cripto- and/or microcrystalline nature of chert accelerates the reaction due to an increase in the surface area available for the reaction. Random microcracking and dissolution can be observed both within and around the boundaries of the particles affected by the alkali–silica reaction [3].

The aim of this study was to investigate the alkali–silica reaction behavior of a chert and the effect of fly ash on the alkali–silica expansion. The study was carried out on mortar bars, which were cast and tested in accordance with an accelerated method, ASTM C1260. The experimental program included measurements of mortar bar expansions, determination of ultrasonic pulse velocity in cracked bars, petrographic analysis of mortar bars, and microscopic examination of the alkali–silica reaction product gel.

2. Materials

The cement used in the study met the ASTM C150 Standard Specification for Type I portland cement. The chemical composition of the cement is shown in Table 1, which also contains the chemical analysis of the fly ash used. The fly ash can be classified as Class F, according to ASTM C618 (i.e., $SiO_2 + Al_2O_3 + Fe_2O_3 \geq 70\%$), although it is obtained from the combustion of a subbituminous coal.

* Corresponding author. Tel.: +90-312-2102429; fax: +90-312-2101262.
E-mail address: turanli@metu.edu.tr (L. Turanli).

0008-8846/$ – see front matter © 2004 Elsevier Ltd. All rights reserved.
doi:10.1016/j.cemconres.2004.02.007

Table 1
Chemical composition of cement and fly ash

	Chemical analysis (%)									
	CaO	SiO_2	Al_2O_3	Fe_2O_3	SO_3	MgO	Na_2O	K_2O	Na_2O_{eq}	LoI
Cement	63.18	19.27	5.59	2.52	3.00	2.77	0.24	1.10	0.96	1.59
Fly ash	13.08	50.48	27.65	4.80	1.30	0.97	0.30	2.00	1.62	1.07

Chert samples were taken from Sogukcam limestone (Cretaceous) near Ankara, Turkey [4]. Within the medium- to thin-bedded beige clayey limestone, chert occurs as nodules or irregular layers with 'pinch and swell' structure. The nodules may be up to 10 cm in length, and the thickness of individual 'bedded cherts' may reach up to 10 cm.

The chert samples are largely composed of microcrystalline quartz with little chalcedony, both existing as small and irregular patches, and scattered calcite crystals. The microcrystalline quartz displays a well-developed mosaic texture. The grain size of the individual crystals ranges from 3 to 12 μm. The limestone used as an inert aggregate in mortar bars is composed of 100% calcite ($CaCO_3$).

3. Experimental study

The experimental program was completed in two series of tests: expansion and sonic velocity measurements of mortar bars containing various amounts of inert limestone and reactive chert in the first series, and the determination of the effect of fly ash on chert at macro- and microlevels in the second series. Eleven sets of mortar bars, each set containing three bars, were cast in accordance with ASTM C1260. Limestone was substituted by chert at 0%, 1%, 3%, 5%, 7.5%, 10%, 15%, 20%, 30%, 50%, and 100% levels in the 11 mixes. The bars were demoulded after 24 h and placed into a water bath at room temperature, then heated to 80 °C, as specified in the test method. The bars were cured for 1 day, then immersed into 1M NaOH solution at 80 °C after the initial (zero day) length measurement. The expansions were recorded thereafter at 3, 7, 14, 21, and 28 days. For the sonic velocity testing, 7-day air-dried bars containing 1%, 3%, 5%, 7.5%, 15%, 50%, and 100% chert were selected, and the longitudinal (P) wave velocities were measured. In the pulse method, an impulse is imparted to the specimens having a length of 80–100 mm, and the time required for the transient pulse to traverse the length of the specimens is used to calculate the velocity of the waves. Pundit plus with P-54 kHz transducers was used for the sonic wave measurements. Thin sections were cut from the same bars used for sonic velocity testing, and examined under polarizing microscope. For the petrographic examination, the number of cracks per unit area, the form, distribution, length and width of cracks across the mortar bar, the type and extent of gel in-filling in cracks and voids, the shape of the aggregates, and the distribution of the voids were evaluated.

In the second part of the program, the aggregate content was fixed as 10% chert and 90% limestone. Four sets of mortar bars to which fly ash was introduced at levels of 10%, 20%, 30%, and 40% cement replacement by mass were cast. The bars were tested in accordance with ASTM C1260, and the expansions were recorded every 3 days up to 30 days. At the end of 30 days, representative samples were cut from the bars, which contained no fly ash (referred to as the control sample) and 40% fly ash. The samples were impregnated with epoxy resin, and their surfaces were polished. Microstructural investigations were carried out using a scanning electron microscope, equipped with energy dispersive X-ray for semiquantitative chemical analysis.

4. Results and discussion

4.1. Determination of chert expansion and sonic velocity

All levels of chert addition led to expansion resulting from the alkali–silica reaction. Fig. 1 shows the expansion curves plotted against the chert content of the mortars. Each curve, from bottom to top, refers to expansion at 3, 7, 14, 21, and 28 days. There is no consistent relationship between chert content and expansion at the end of the first week. However, the relation became obvious starting at 14 days. The hump in the expansion curve lying between the range of 5–15% chert content is apparent. At 28 days, expansions of the bars containing 5%, 7.5%, 10%, and 15% chert were 0.23%, 0.25%, 0.26%, and 0.24%, respectively. Although the peak seems to be centered at 10% chert content, the values are close to each other. This phenomenon is the well-known 'concept of pessimum' or 'pessimal proportion' [5]. As the percentage of reactive constituent increases, expansion increases up to a certain percentage of reactive material and decreases after that level. This peak percentage is named the pessimum proportion; however, many aggregates, especially slow-reacting ones, do not exhibit pessimum behavior. It is believed

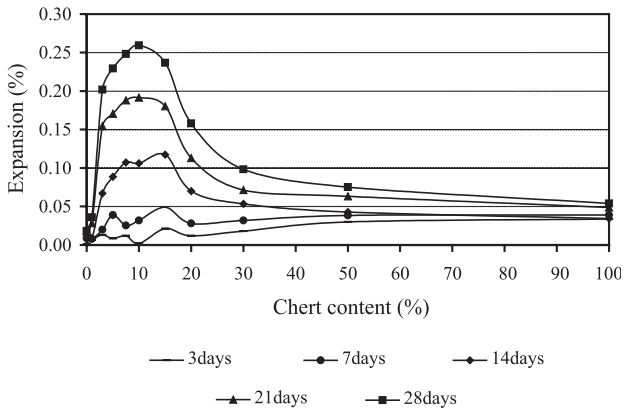

Fig. 1. Pessimum behavior of chert.

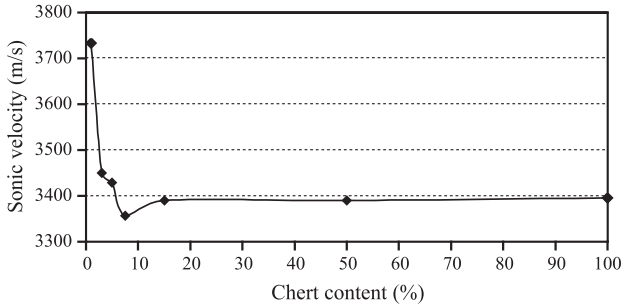

Fig. 2. Sonic velocities of the bars containing various amounts of chert.

that the pessimum proportion depends on the reactivity of the aggregate. As reactivity increases, the pessimum proportion shifts to the left on the percent scale; in other words, more reactive aggregates show the maximum expansion at lower percentages. It is stated that there is a critical ratio of alkali-to-reactive silica to cause deleterious expansion. When the reactive aggregate content is too high, the alkali is used up rapidly, and the reaction product is nonexpanding or does not expand enough to cause deleterious expansion [6]. However, this explanation fails in the accelerated method because alkali supply can be considered as infinite. The authors believe that this phenomenon merits further study to be clarified. Another point is whether large proportions of chert, i.e., >50%, can be used without any risk of deleterious expansion or not. ASTM C33 limits chert content to 8% and 3% for fine and coarse concrete aggregate, respectively. However, the results showed that the bars containing 50% and 100% chert expand 0.08% and 0.05%, respectively, even at 28 days. These values are below the limit of 0.10% expansion at 14 days recommended by ASTM C1260.

Measurement of ultrasonic pulse velocity in damaged concrete is a common nondestructive method to find out the degree of cracking. This method has also been used to assess the cracking due to alkali–silica reaction. Sonic velocity decreases as cracking increases. The variation of the sonic wave velocity of the dry mortar bars for various chert contents is plotted in Fig. 2. The results are in good agreement with the expansions observed. The sonic velocity decreased as the chert content increased up to 8–9%, and it slightly increased after this point as the chert content increased. The significant decrease in sonic velocity can be attributed to cracking due to ASR. The sonic velocity results confirm the expansion results stating that the maximum cracking occurred in between the 5–15% range of chert content.

4.2. Petrographic examination

Various properties related to cracks, voids, and aggregates were determined by petrographic examination. Table 2 summarizes the petrographic properties of the bars for various chert contents. The variation of the number of cracks with chert content (Fig. 3a) indicates that the number increases as the chert content increases and reaches a maximum value at 7.5%. However, it decreases as the chert content further increases. The length of cracks versus chert graph (Fig. 3b) also gave a similar plot. These relationships are consistent with expansion and sonic velocity results. On the other hand, the width of cracks fluctuates with increasing chert content, although the peak value corresponds to 7.5% (Fig. 3c).

The petrographic study also indicated that the alkali–silica reaction caused radial cracking and rim formation around cherts, with or without cracking in the mortar bars, at almost all chert contents under investigation.

4.3. Fly-ash addition and microstructural study

Limestone and chert were blended together at a ratio of 9:1 to attain the maximum expansion in the mortar bar test. Fig. 4 shows the expansion values of specimens containing

Table 2
Results of petrographic examination after 28 days of exposure

	Chert content (%)						
	1	3	5	7.5	15	50	100
Number of cracks (per mm^2)	0.11	0.13	0.16	0.24	0.17	0.11	0.07
Length of cracks (mm)	0.125–0.450	0.125–3.500	0.250–5.750	0.750–12.500	0.250–5.250	0.125–0.250	0.125–0.375
Width of cracks (mm)	0.0075–0.0750	0.0075–0.0125	0.0125–0.0375	0.0050–0.1250	0.0125–0.0500	0.0075–0.0125	0.0075–0.0250
Air voids (%)	15	15	15	15	15	15	15
Gel-filling air voids (%)	0	5	7	9	10	6	1
Gel-filling cracks	100	100	100	100	100	100	100
Crack forms	Radial cracking, especially around air voids	Rim with cracking and radial cracking	Rim with cracking and radial cracking	Rim with cracking and radial cracking	Rim with cracking and radial cracking	Rim with cracking and radial cracking	Random cracking
Shape of aggregates	Angular	Subangular to angular	Angular	Angular	Angular	Angular	Angular

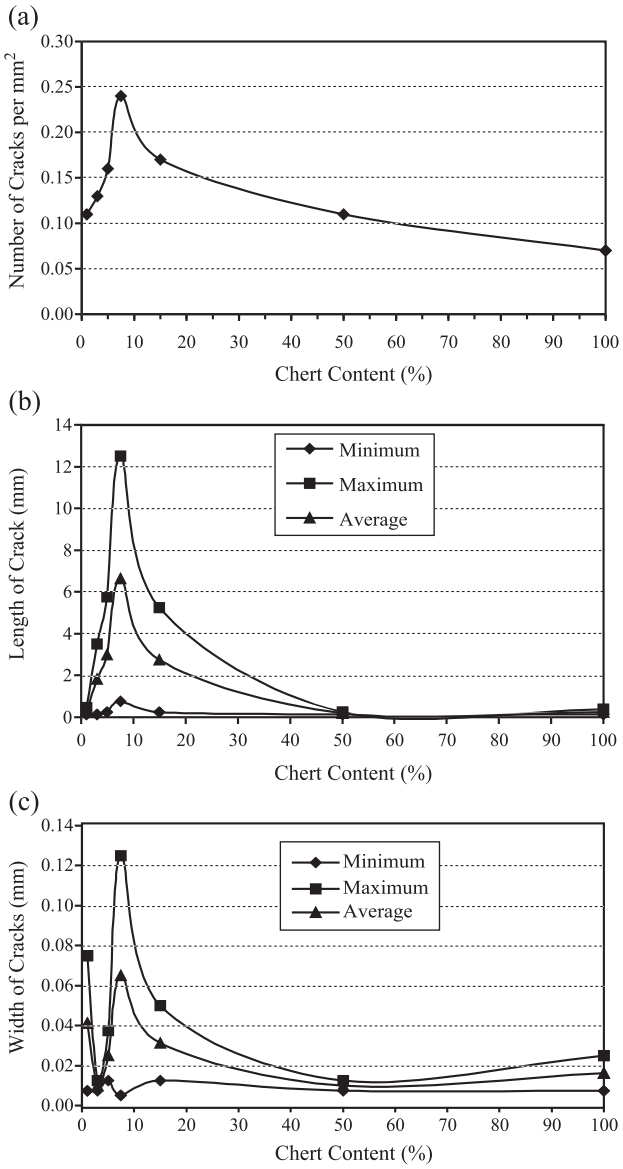

Fig. 3. Graphical interpretation of the crack analysis of thin-sections-plotted chert content versus (a) number of cracks per mm^2, (b) length of cracks, and (c) width of cracks.

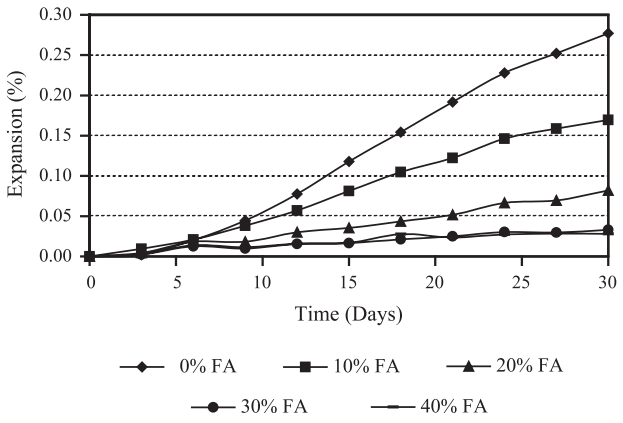

Fig. 4. Expansions of mortar bars containing fly ash (FA: fly ash).

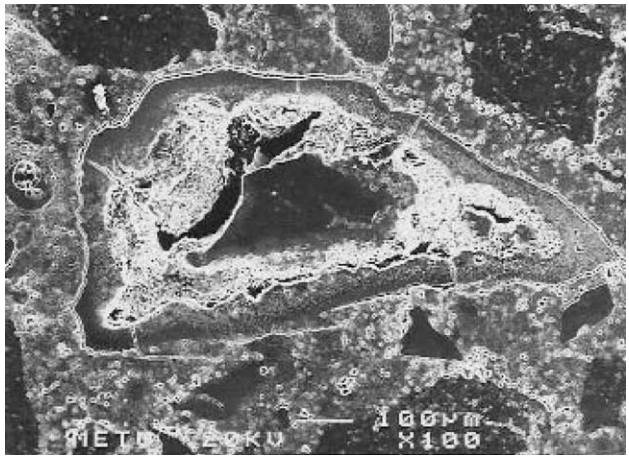

Fig. 5. Alkali–silica reaction initiated within the chert particle.

0% (control), 10%, 20%, 30%, and 40% fly-ash substitution for cement. It is obvious from the figure that all replacement levels reduced the expansion compared with the control specimens. At the end of 30 days, the length changes monitored were 0.28%, 0.17%, 0.08%, 0.03%, and 0.03% for the control specimens, 10%, 20%, 30%, and 40% fly ash replacements, respectively. The expansion decreased as the fly-ash amount increased. It is worth noting that the reductions achieved by 30% and 40% fly ash were dramatic, corresponding to 89% reduction for both when compared with the control specimens.

The suppressing effect of fly ash on alkali–silica expansion is attributed to the following factors: (1) dilution effect, the reduction in the amount of cement alkali; (2) reduced permeability thus limited ionic mobility; (3) consumption of $Ca(OH)_2$, leading to a decreased amount of hydroxyl ions to attack silica; and (4) entrapment of alkalis in the hydration products of fly ash. In fact, there is not a solid consensus on the phenomenon. The mechanism may be a combination of all the factors listed above. It is worth noting that the fly ash used in the study was effective at relatively low levels

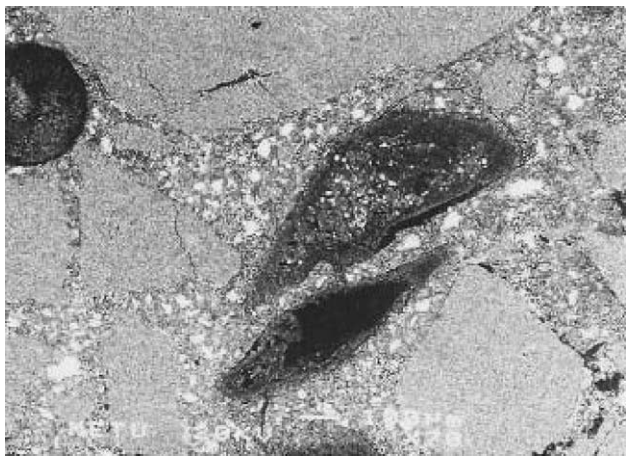

Fig. 6. BEI image of reacted chert particles transformed into gel.

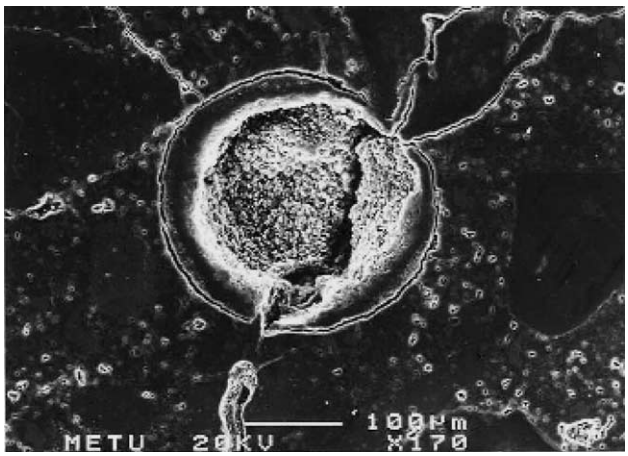

Fig. 7. Alkali–silica gel deposit with crystallised surface.

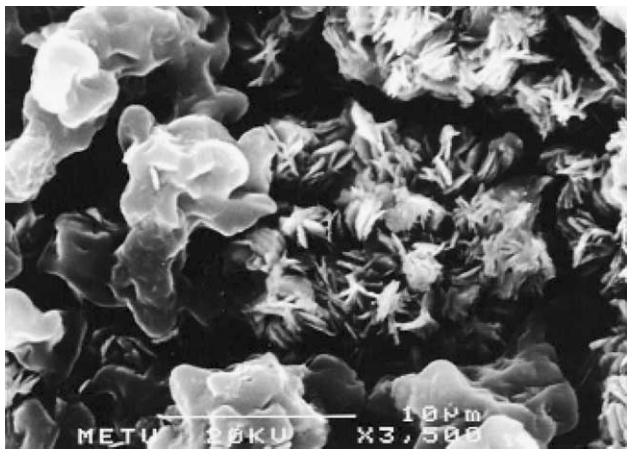

Fig. 9. Lamella crystals similar with rosette-like morphology.

although it is a moderate-calcium fly ash. Generally, it is believed that the higher the CaO content of fly ash, the less effective it is in mitigating expansion due to alkali–silica reaction. Shehata and Thomas [7] showed that the efficacy of fly ash was reduced significantly when its CaO content is higher than 20%.

At the end of 30-day period, characteristic map cracking was more prominent on the surface of the control bars. The microstructural investigations confirmed the visual inspection. Internal cracking was present both in the control and 40% fly ash samples but was more intense in the control. Bonding between the reacted particles and the cement matrix was disturbed due to expansive forces created by the reaction. The opening surrounding the particle is clearly seen in Fig. 5. For the same figure, it is understood that the dissolution of the reactive silica began within the particle. Probably, the porous structure of chert gave rise to this kind of initiation. Fig. 6 is a backscattered image taken from the control sample. The particles at the center of the figure were transformed to alkali–silica gel. Expansive forces not only cracked the reactive aggregate particles but also cracked the inert limestone particles and the surrounding cement paste.

Alkali–silica gel was identified in cracks in the aggregate particles, in the cement paste, and in the air voids as lining or filling up parts of the void (Figs. 7 and 8). The detection of gel in the cracks and voids implies that there was a gel flow from the reaction sites to the cement matrix. Bleszynski and Thomas stated that the gel is relatively fluid and readily disperses into the cement paste when it is low in calcium and high in alkali, just at the end of the reaction [8]. The alkali–silica gel deposits found in the control sample exhibited a crystallized surface. Rosette-like lamella crystals can be seen in Fig. 9. It was observed that the surface of the gel deposits of the sample containing fly ash developed a spongy layer, which is rich in calcium (Fig. 10). The source of the calcium ions might be the limestone used or the cement paste. Large drying cracks were monitored on the surface of this layer (Fig. 8). Regourd and Hornain [9] stated that with time, massive gel deposits might develop a texture, grainy, spongy, or foliated, always related to an increase in calcium ions.

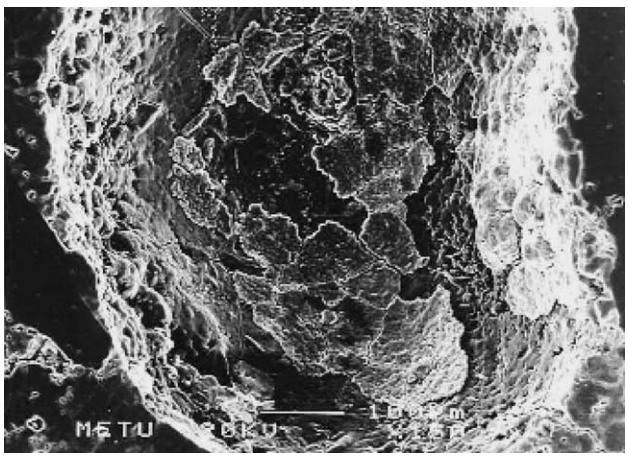

Fig. 8. Drying cracks on the alkali–silica gel.

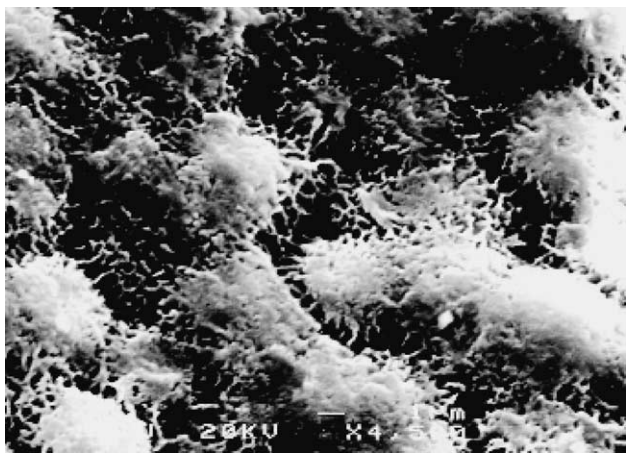

Fig. 10. Spongy texture exhibited by the gel.

Table 3
Chemical composition of the alkali–silica gels

	SiO_2	CaO	Na_2O	K_2O	Al_2O_3	Na_2O_{eq}	CaO/Na_2O_{eq}
Control sample							
Gel 1	64.41	14.01	20.96	0.63	0.00	21.37	0.66
Gel 2	63.66	11.87	24.20	0.28	0.00	24.38	0.49
Gel 3	71.42	10.25	17.65	0.67	0.00	18.09	0.57
Gel 4	57.67	18.63	19.46	1.09	3.15	20.18	0.92
Gel 5	62.74	11.29	24.58	0.96	0.00	25.21	0.45
Fly-ash sample (40%)							
Gel 1	47.79	29.26	16.08	1.22	4.32	16.88	1.73
Gel 2	51.45	29.03	15.62	1.41	2.06	16.55	1.75
Gel 3	60.76	15.72	7.95	3.22	11.25	10.07	1.56
Gel 4	53.34	22.32	15.64	4.60	0.56	18.67	1.20

Table 3 shows the point analyses of alkali–silica gels detected in different reaction sites of the control and the fly-ash-rich samples. The chemical composition of the two groups of gels differed in calcium contents: The calcium content of the control sample gels was higher compared with that of the fly-ash sample gels. The CaO/Na_2O_{eq} of the fly-ash sample gels is between 1.20 and 1.75, whereas this ratio is 0.45–0.92 for the control sample gels. That is, as the CaO/Na_2O_{eq} of the gel increased, the expansion decreased. This result is consistent with the previous studies in which the expansion mechanism of alkali–silica gel was attributed to swelling caused by electrical double-layer repulsion forces. Prezzi et al. [10] postulated that the reaction product gels containing larger amounts of Na_2O_{eq} and smaller CaO/Na_2O_{eq} cause larger expansions. In the second part of their study, carried out with different chloride salts, Prezzi et al. [11] found that monovalent cations, i.e., Na, K, Li, present in alkali–silica gel lead to higher pressures compared with other ions of higher valance, i.e., Ca, Mg, Al.

5. Conclusion

The alkali-reactive chert used in the study showed pessimum proportion behavior. The pessimum content of this chert lies in the range of 5–15%. The expansion caused by alkali–silica reaction increased up to the level mentioned above and decreased after this range. The study showed that high proportions of chert in the aggregate, i.e., >50%, did not result in deleterious expansion. These results obtained by mortar bar and ultrasonic velocity tests were confirmed by petrographic examination. As the fly-ash replacement increased, the expansion experienced by the bars decreased. Relatively low levels of moderate-calcium fly ash reduced the expansion below the critical limit of 0.10% recommended by ASTM C1260. The authors believe that further studies are needed to evaluate the efficacy of moderate-calcium fly ashes on alkali–silica reaction. Microstructural observations were in good agreement with the double-layer theory, which was proposed to explain the expansion mechanism of alkali–silica gel. As the CaO/Na_2O_{eq} of alkali–silica gel increases, the expansivity of the gel decreases.

The preliminary results given in this paper only regard a specific type of chert. Further investigations are being carried out in cherts having different mineralogical–textural features, and this may lead to a better understanding of the ASR phenomenon involving chert.

Acknowledgements

The authors would like to thank Professor P. Kumar Mehta for his valuable comments on the study.

References

[1] R.N. Swamy (Ed.), The Alkali–Silica Reaction in Concrete, Blackie and Son, Glasgow, 1992, pp. 128, 234, 273.
[2] H. Williams, F.J. Turner, C.H. Gilbert, Petrography, Freeman, New York, USA, 1982.
[3] B.J. Wigum, Alkali–Aggregate Reactions in Concrete: Properties, Testing and Classification of Norwegian Cataclastic Rocks, PhD dissertation, University of Trondheim, Norway, 1995.
[4] M.C. Goncuoglu, N. Turhan, K. Senturk, A geotraverse across NW Turkey: tectonic units of the Central Sakarya region and their tectonic evolution, Spec. Publ.-Geol. Soc. Lond. 173 (2000) 139–161.
[5] D.W. Hobbs, Expansion of concrete due to alkali–silica reaction: an explanation, Mag. Concr. Res. 30 (105) (1978) 215–220.
[6] H. Xu, On the alkali content of cement in AAR, in: P.E. Grattan-Bellew (Ed.), Proceedings of the 7th International Conference, 1986, Ottowa, Canada, Noyes Publications, New Jersey, USA, 1987, pp. 451–455.
[7] M.H. Shehata, M.D.A. Thomas, The effect of fly ash composition on the expansion of concrete due to alkali–silica reaction, Cem. Concr. Res. 30 (2000) 1063–1072.
[8] R.F. Bleszynski, M.D.A. Thomas, Microstructural studies of alkali–silica reaction in fly ash concrete immersed in alkaline solution, Adv. Cem. Based Mater. 7 (1998) 66–78.
[9] M. Regourd, H. Hornain, Microstructure of reaction products, in: P.E. Grattan-Bellew (Ed.), Proceedings of the 7th International Conference, 1986, Ottowa, Canada, Noyes Publications, New Jersey, USA, 1987, pp. 375–380.
[10] M. Prezzi, P.J.M. Monteiro, G. Sposito, The alkali–silica reaction: Part I. Use of the double-layer theory to explain the behavior of reaction-product gels, ACI Mater. J. 94 (1) (1997) 10–17.
[11] M. Prezzi, P.J.M. Monteiro, G. Sposito, The alkali–silica reaction: Part II. The effect of chemical admixtures, ACI Mater. J. 95 (1) (1998) 3–10.